Leptin's hunger-suppressing effects are mediated by the hypothalamic–pituitary–adrenocortical axis in rodents

Rachel J. Perry[a,b,1], Jon M. Resch[c,1], Amelia M. Douglass[c,1], Joseph C. Madara[c], Aviva Rabin-Court[a], Hakan Kucukdereli[c], Chen Wu[c], Joongyu D. Song[a], Bradford B. Lowell[c,d,2], and Gerald I. Shulman[a,b,2]

[a]Department of Internal Medicine, Yale University School of Medicine, New Haven, CT 06520; [b]Department of Cellular and Molecular Physiology, Yale University School of Medicine, New Haven, CT 06520; [c]Division of Endocrinology, Diabetes, and Metabolism, Department of Medicine, Beth Israel Deaconess Medical Center, Harvard Medical School, Boston, MA 02215; and [d]Program in Neuroscience, Harvard Medical School, Boston, MA 02215

Contributed by Gerald I. Shulman, May 20, 2019 (sent for review February 4, 2019; reviewed by Roger D. Cone and Richard D. Palmiter)

Leptin informs the brain about sufficiency of fuel stores. When insufficient, leptin levels fall, triggering compensatory increases in appetite. Falling leptin is first sensed by hypothalamic neurons, which then initiate adaptive responses. With regard to hunger, it is thought that leptin-sensing neurons work entirely via circuits within the central nervous system (CNS). Very unexpectedly, however, we now show this is not the case. Instead, stimulation of hunger requires an intervening endocrine step, namely activation of the hypothalamic–pituitary–adrenocortical (HPA) axis. Increased corticosterone then activates AgRP neurons to fully increase hunger. Importantly, this is true for 2 forms of low leptin-induced hunger, fasting and poorly controlled type 1 diabetes. Hypoglycemia, which also stimulates hunger by activating CNS neurons, albeit independently of leptin, similarly recruits and requires this pathway by which HPA axis activity stimulates AgRP neurons. Thus, HPA axis regulation of AgRP neurons is a previously underappreciated step in homeostatic regulation of hunger.

leptin | food intake | corticosterone | obesity | AgRP neurons

Since the discovery of leptin, it has been known that leptin deficiency causes unrestrained appetite and, consequently, hyperphagia leading to obesity, insulin resistance, and type 2 diabetes (1–4). In contrast, leptin treatment in overweight humans and rodents, who tend to exhibit hyperleptinemia at baseline, has been shown to have little to no impact on food intake, body weight, or insulin sensitivity (5–7) except in the rare individuals with markedly low, absent, or nonfunctional leptin (8–13). These data suggest that leptin is of greatest physiologic importance in modulating food intake in the low to normal range, as a response to starvation, while, in contrast, increases from the normal to high range are of minimal physiologic importance.

Leptin initiates its effects by engaging leptin receptors on hypothalamic neurons. Indeed, deletion of leptin receptors from hypothalamic (14), GABAergic (15), neuronal nitric oxide synthase (*Nos1*)-expressing (16), or agouti-related peptide (AgRP)-expressing neurons (17) causes hyperphagia and massive obesity indicating that leptin signaling in these neurons is necessary for the regulation of food intake. While the definitive neuronal mechanism by which hypoleptinemia promotes hyperphagia has not been conclusively established, it is likely to involve both direct and indirect (via intervening neurons) stimulation of AgRP neurons and inhibition of POMC neurons in the arcuate nuclei of the hypothalamus, with both actions converging to increase hunger.

In addition, the mechanism by which hypercorticosteronemia stimulates food intake remains unknown. Potential mediators of this response are AgRP neurons within the arcuate nucleus of the hypothalamus. AgRP neurons are an integral component of appetite regulation, having been shown to be sufficient to drive feeding behavior (18, 19). These cells express glucocorticoid receptors (20, 21), and corticosterone has been shown to regulate expression of the orexigenic peptides expressed by these neurons, AgRP and neuropeptide Y (NPY) (22–24). Here, we show that hypoleptinemia activates the hypothalamic–pituitary–adrenocortical (HPA) axis under conditions of starvation and poorly controlled type 1 diabetes (T1D), and that hypercorticosteronemia is both necessary and sufficient to drive hyperphagia during starvation and T1D. Finally, we examine the mechanism by which hypercorticosteronemia promotes hyperphagia under these conditions and demonstrate that hyperphagia is mediated through corticosterone acting directly on AgRP neurons to stimulate their activity.

Results

Hypoleptinemia-Mediated HPA Axis Activation Causes Hyperphagia in Starvation and Poorly Controlled T1D. After a 48-h fast, rats were hypoleptinemic and hypercorticosteronemic. Hypercorticosteronemia caused hyperphagia: 48-h–fasted rats consumed 14 times more chow upon refeeding compared with their 6-h–fasted counterparts, while intraarterial infusion of corticosterone to match plasma corticosterone concentrations to those measured in 48-h–fasted rats largely replicated the hyperphagic effect of starvation. In contrast, normalizing plasma leptin concentrations with a 6-h leptin infusion suppressed food intake through a corticosterone-dependent mechanism, as demonstrated by the fact that restoring hypercorticosteronemia in leptin-infused rats abrogated the effect of leptin to suppress food intake. Finally, treatment with a glucocorticoid

Significance

Low levels of leptin, a hormone secreted by adipocytes that signals the body as to the availability of fuel stores, are known to increase food intake. Here, we demonstrate a mechanism by which low leptin stimulates food intake in rodents: Under conditions of hypoleptinemia, stress hormone (glucocorticoid) production is increased, and in turn stimulates AgRP neurons to promote appetite.

Author contributions: R.J.P., J.M.R., A.M.D., B.B.L., and G.I.S. designed research; R.J.P., J.M.R., A.M.D., J.C.M., A.R.-C., H.K., C.W., and J.D.S. performed research; R.J.P., J.M.R., A.M.D., J.C.M., A.R.-C., H.K., C.W., J.D.S., B.B.L., and G.I.S. analyzed data; and R.J.P., J.M.R., A.M.D., B.B.L., and G.I.S. wrote the paper.

Reviewers: R.D.C., University of Michigan; and R.D.P., University of Washington.

Conflict of interest statement: G.I.S. is on the Scientific Advisory Boards for Merck, NovoNordisk, AstraZeneca, Aegerion, iMBP, and Jansen Research and Development, and receives investigator-initiated support from Gilead Sciences and Merck. R.J.P. and G.I.S. receive investigator-initiated support from AstraZeneca. All other authors declare no competing interests.

[1]R.J.P., J.M.R., and A.M.D. contributed equally to this work.

[2]To whom correspondence may be addressed. Email: blowell@bidmc.harvard.edu or gerald.shulman@yale.edu.

This article contains supporting information online at www.pnas.org/lookup/suppl/doi:10.1073/pnas.1901795116/-/DCSupplemental.

Published online June 18, 2019.

receptor antagonist, mifepristone, suppressed caloric intake to that measured in recently fed animals without altering plasma leptin concentrations. Plasma adrenocorticotropic hormone (ACTH) concentrations mirrored plasma corticosterone, with the exception of mifepristone-treated rats, which exhibited the expected increase in ACTH resulting from glucocorticoid receptor antagonism. Taken together, these data suggest that hypercorticosteronemia mediates the majority of fasting-induced hyperphagia (Fig. 1 *A–C* and *SI Appendix*, Fig. S1 *A–F*). Next, we performed similar studies in insulin-deficient, poorly controlled type 1 diabetic rats, as we and others have shown that poorly controlled diabetes is a state of severe hypoleptinemia (25–33). In this model, we again found that hypoleptinemia caused hypercorticosteronemia in T1D rats as replacement leptin normalized plasma corticosterone concentrations and reversed hyperglycemia without affecting plasma insulin concentrations. Hypoleptinemia caused hyperphagia in T1D rats, an effect mediated through hypercorticosteronemia: Animals with poorly controlled T1D consumed twice as many calories within a 2-h span compared with nondiabetic rats, an observation corrected by replacement leptin infusion and restored by coinfusion of corticosterone

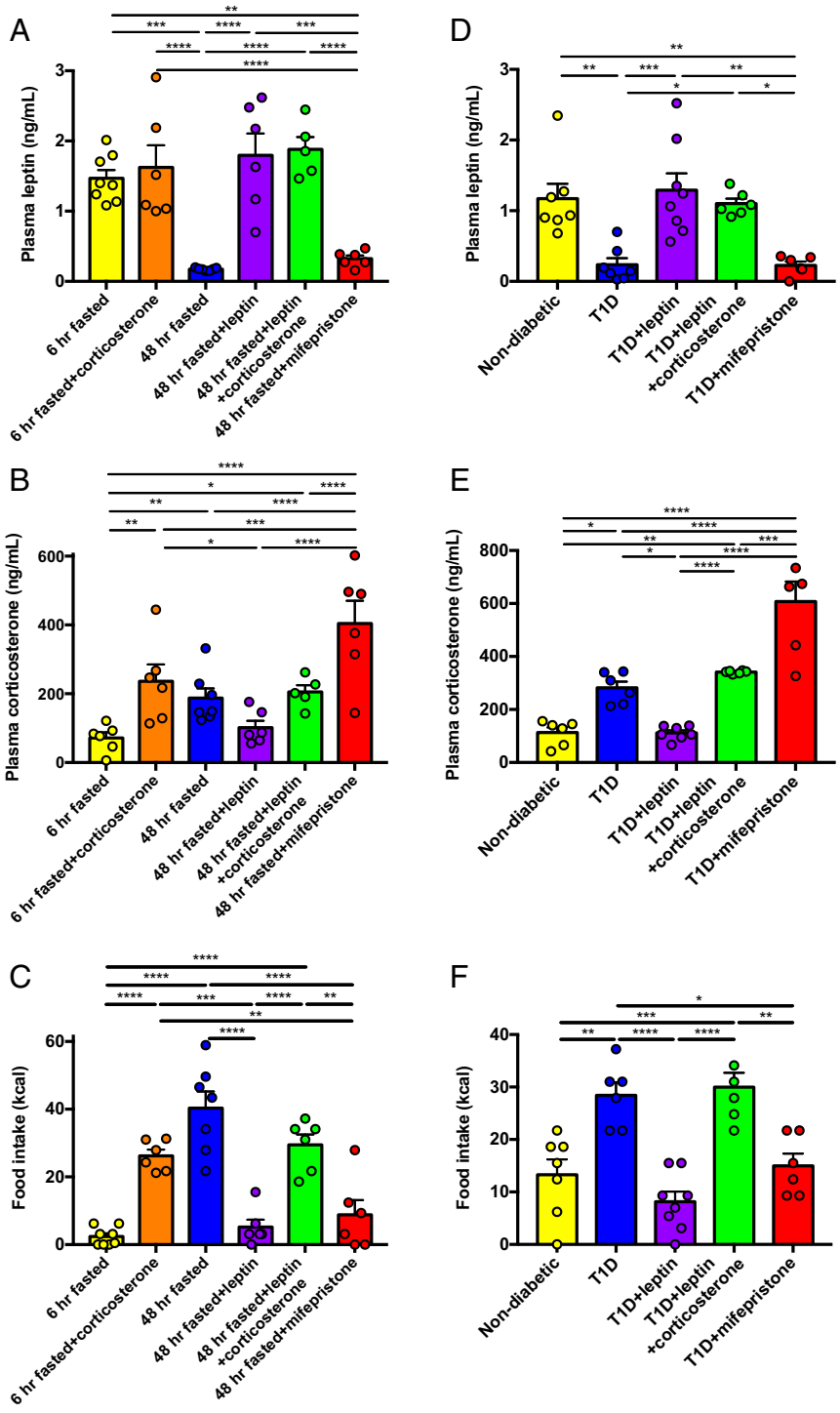

Fig. 1. Hypoleptinemia-mediated hypercorticosteronemia causes hyperphagia in fasted and type 1 diabetic rats. (*A* and *B*) Plasma leptin and corticosterone in healthy rats after 4 h of infusion, before refeeding. (*C*) Food intake measured over a 2-h period. (*D* and *E*) Plasma leptin and corticosterone in healthy and type 1 diabetic rats after 4 h of infusion, before refeeding. (*F*) Food intake measured over 2 h. In all panels, $*P < 0.05$, $**P < 0.01$, $***P < 0.001$, and $****P < 0.0001$ by one-way ANOVA with Bonferroni's multiple-comparisons test. Data are the mean ± SEM.

in rats treated with leptin. Mifepristone treatment abrogated the effect of poorly controlled diabetes to cause hyperphagia, suppressing food intake after an overnight fast to rates measured in nondiabetic controls (Fig. 2 *A–C* and *SI Appendix*, Fig. S2 *A–F*).

HPA Axis Activation Causes Hyperphagia in Hypoglycemia. We next hypothesized that HPA axis activation would drive hyperphagia during acute, insulin-induced hypoglycemia (34). Consistent with this, following a 4-h hyperinsulinemic–hypoglycemic clamp, rats consumed 4 times as many calories as euglycemic rats infused with the same dose of insulin, despite unchanged plasma leptin concentrations. The majority of this hyperphagia was driven by hypercorticosteronemia, as evidenced by the fact that infusing euglycemic rats with corticosterone to increase plasma corticosterone concentrations to levels measured in hypoglycemic rats recapitulated the majority of the effect of hypoglycemia to cause hyperphagia. In contrast, mifepristone treatment reduced food intake in hypoglycemic rats to rates measured under euglycemic conditions (Fig. 3 *A–C* and *SI Appendix*, Fig. S3 *A–F*), thereby demonstrating that hypercorticosteronemia, and not central hypoglycemia, is ultimately responsible for the majority of hypoglycemia-induced hyperphagia.

Elevated Leptin Abrogates HPA Axis-Mediated Hyperphagia. To directly test the role of corticosterone in modulating food intake, we studied adrenalectomized (ADX) mice infused with low (0.75 mg/d) or high (2 mg/d) doses of corticosterone s.c. Corticosterone drove food intake: Both total caloric intake and caloric intake following a 24-h fast were reduced in the ADX-low corticosterone group, and increased to control rates in ADX-high corticosterone-treated mice (*SI Appendix*, Fig. S4 *A–D*). We then placed the ADX mice on a high-fat diet (HFD) for 2 wk to test whether increased adiposity may prevent hyperphagia after a fast. High-fat feeding more than doubled fat mass and reduced caloric intake upon refeeding by 40% only in sham-operated mice (*SI Appendix*, Fig. S4 *E–H*). Given the decreased food intake after a fast in sham-operated mice fed an HFD, these data suggest that obesity generates a negative-feedback signal dependent on glucocorticoid activity to suppress fasting-induced hyperphagia.

We tested this hypothesis in ADX rats, which, unlike mice, afford the ability to measure plasma glucocorticoid concentrations in the unrestrained, awake state. In ADX rats, fasting lowered leptin and refeeding increased it independent of adrenal function. However, corticosterone drove fasting-induced hyperphagia: Upon refeeding, 24-h–fasted ADX-low corticosterone-treated rats exhibited a 50% reduction in caloric intake compared with both sham-operated and high-corticosterone treated ADX rats. After 10 d of high-fat feeding, plasma leptin concentrations increased: After a 24-h fast, plasma leptin concentrations dropped only to ∼2 ng/mL, compared with 0.5 ng/mL in chow-fed rats. This increase in plasma leptin concentrations prevented the fasting-induced increase in plasma corticosterone in sham-operated rats, and consequently reduced food intake after a 24-h fast to levels measured in ADX-low corticosterone-treated rats (Fig. 3 *A–F* and *SI Appendix*, Fig. S5 *A–D*).

Correcting Body Weight in Obese Rodents Restores Fasting-Induced Hyperphagia. Because these data demonstrate that elevated leptin reduced fasting-induced hypoleptinemia and consequently abrogated hypercorticosteronemia-mediated hyperphagia in the fasted–refed state, we next sought to determine whether these alterations could be reversed by normalizing body weight in rats with diet-induced obesity. To that end, we placed 4-wk HFD rats on a very-low–calorie diet (VLCD) (10.4 kcal/d, ∼20% of their typical daily caloric intake) to reduce their body weight to that of healthy rats. This intervention lowered plasma leptin and increased plasma corticosterone during a 48-h fast to those of lean rats, resulting in a 3.5-fold increase in food intake upon refeeding (Fig. 3 *G–I* and *SI Appendix*, Fig. S6 *A–C*), suggesting a threshold for plasma leptin at which the HPA axis and, consequently, hyperphagia are activated.

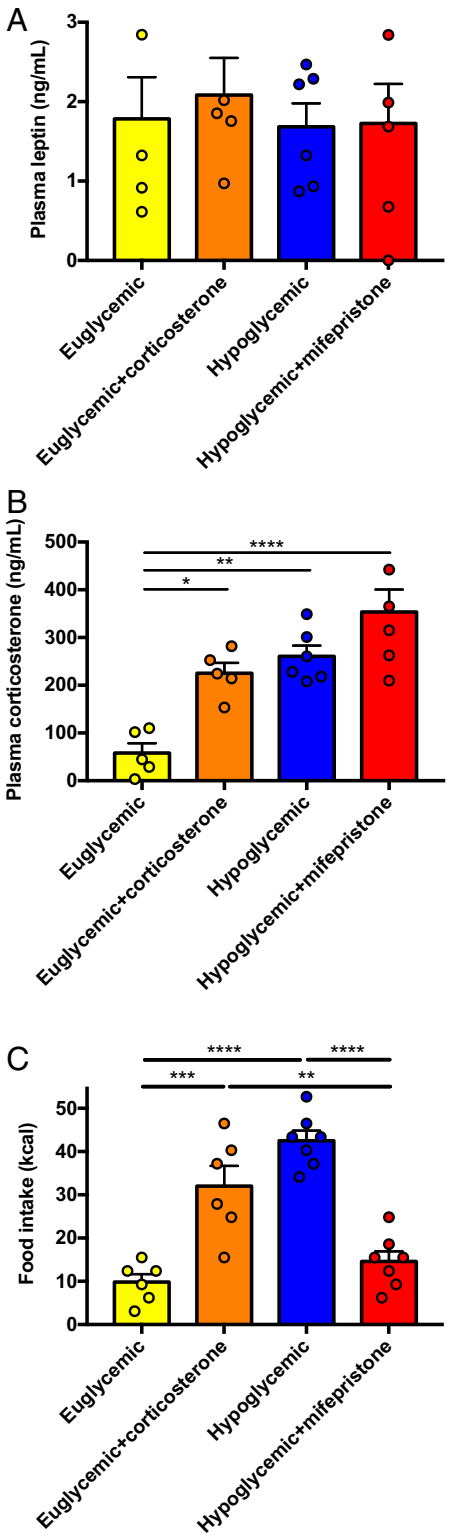

Fig. 2. Hypercorticosteronemia, independent of leptin, causes hyperphagia in insulin-induced hypoglycemia. (*A* and *B*) Plasma leptin and corticosterone after 4 h of infusion, before refeeding. (*C*) Food intake measured over 2 h. $*P < 0.05$, $**P < 0.01$, $***P < 0.001$, and $****P < 0.0001$ by one-way ANOVA with Bonferroni's multiple-comparisons test. Data are the mean ± SEM.

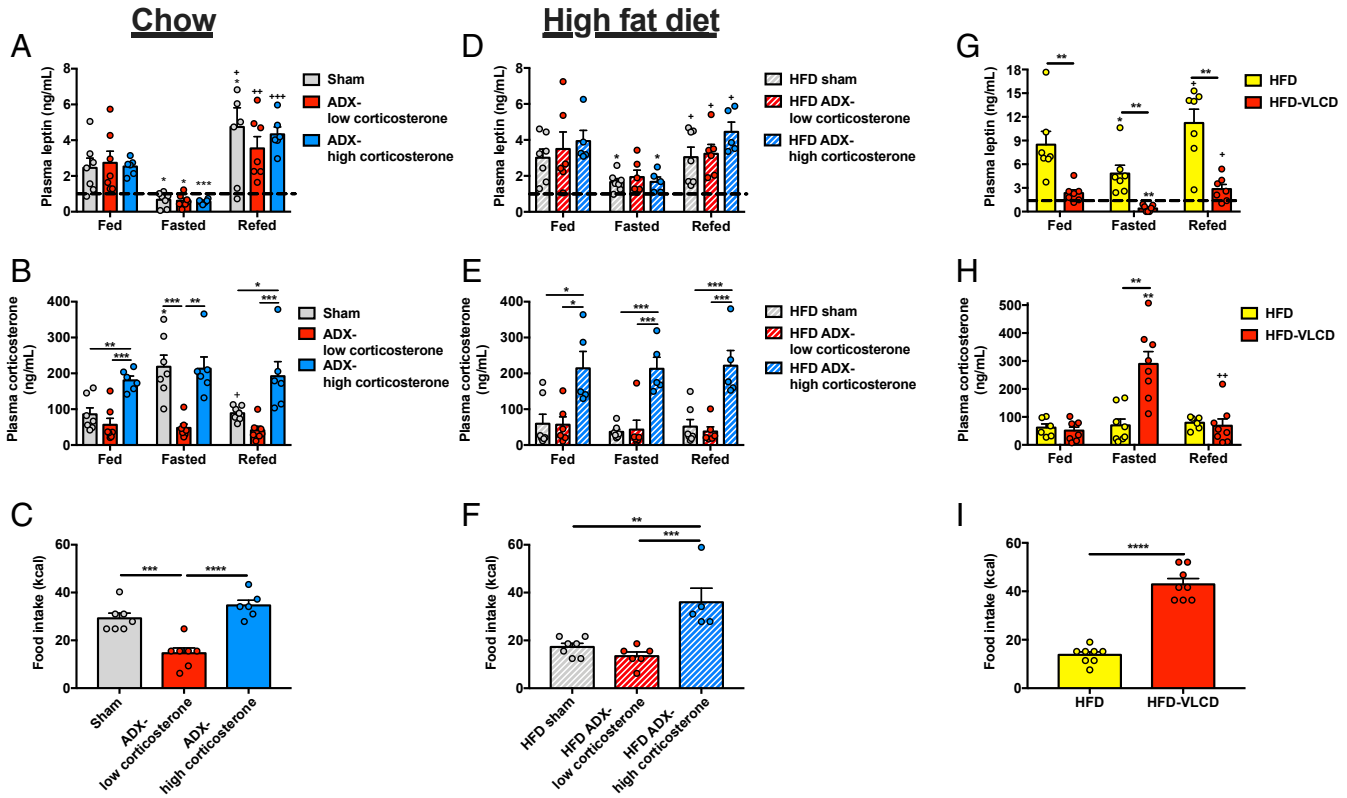

Fig. 3. Elevated leptin abrogates HPA axis-mediated hyperphagia. (*A* and *B*) Plasma leptin and corticosterone in chow-fed rats. (*C*) Food intake after 48-h food withdrawal. (*D–F*) Plasma leptin and corticosterone and refed food intake in 2-wk HFD rats. (*G* and *H*) Plasma leptin and corticosterone in HFD rats before and after a VLCD to normalize body weight. (*I*) Food intake. In all panels, $^{*}P < 0.05$, $^{**}P < 0.01$, and $^{***}P < 0.001$ between the groups designated or, in the case of symbols over individual bars, versus the same group, fed. $^{+}P < 0.05$, $^{++}P < 0.01$, and $^{+++}P < 0.001$ versus the same group, fasted. In all panels, different groups were compared by one-way ANOVA with Bonferroni's multiple-comparisons test, while the same group was compared at different feeding time points by paired ANOVA (*A–F*) while HFD vs. HFD-VLCD rats were compared at the same fasting time point by paired *t* test. Data are the mean ± SEM of $n = 8$ per group.

Corticosterone Increases the Activity of AgRP Neurons. Because genetic tools in mice more readily allow for a mechanistic examination of neural processes, we next set out to confirm a similar role for corticosterone in modulating feeding behavior in mice. We therefore assessed the effect of elevated corticosterone on food intake in mice. To do so, slow-release corticosterone or placebo pellets were implanted subcutaneously 2 h prior to dark cycle onset. As a consequence, mice that received corticosterone pellets should have elevated corticosterone in the following light period, compared with placebo-implanted animals, in which corticosterone is at its circadian nadir (35–38) (Fig. 4*A*). Indeed, corticosterone implants significantly increased plasma corticosterone to levels similar to previous reports in fasted mice (36) and our starvation, T1D, hypoglycemia, and corticosterone infusion studies in rats (Fig. 4*B*; see Figs. 1–3). Food intake in the early light period was also significantly increased (Fig. 4*C*), while food intake in the preceding dark cycle, when corticosterone is naturally high, was comparable to placebo-implanted animals (*SI Appendix*, Fig. S7*A*). These data confirm that corticosterone treatment is sufficient to drive food intake in mice under ad libitum conditions.

We next investigated the neural mechanism underlying the corticosterone-mediated increase in food intake. Given the importance of AgRP neurons for feeding behavior and that their firing pattern closely reflects circadian (39, 40) and starvation-induced fluctuations in corticosterone (41–43), a potential mechanism by which corticosterone drives feeding is by acting on AgRP neurons to increase their activity. We therefore performed ex vivo cell-attached recordings from AgRP neurons under 2 conditions in which corticosterone levels are high, concomitant with an increase in appetite. AgRP neurons were identified in ex vivo brain slices for electrophysiology studies by using *Npy*-hrGFP mice (44) (Fig. 4*D*). First, we confirmed previous findings that AgRP neurons fire with higher frequency in the fasted state (41–43) (Fig. 4 *E* and *F*). This effect persisted in the presence of blockers of AMPA, kainate, NMDA, and GABA-A receptor-mediated synaptic transmission, suggesting a cell-autonomous component to their firing under caloric deficit. Second, we assessed whether administering exogenous corticosterone to mice would increase the firing rate of AgRP neurons. We therefore implanted placebo or corticosterone pellets into *Npy*-hrGFP mice (as in Fig. 4*A*), and mice were killed for electrophysiology recordings 2 h into the following light period when corticosterone levels are naturally low. AgRP neuron firing rates were significantly higher in mice that received corticosterone pellets, which persisted in the presence of synaptic blockers (Fig. 4 *G* and *H*). Exogenous corticosterone administration did not have an effect on the firing of *Npy*-hrGFP–negative neurons in the arcuate (Fig. 4*I*).

To further examine the effect of corticosterone on AgRP neuron firing, we assessed whether corticosterone increases the activity of AgRP neurons in vivo. To do so, we virally expressed the Ca^{2+} sensor, GCaMP6s, in AgRP neurons using *Agrp*-IRES-Cre mice (45) and performed fiber photometry recordings in the early light cycle in awake, behaving mice (46) (Fig. 4*J*). Subcutaneous injection of corticosterone (2 mg/kg) significantly increased AgRP neuron activity compared with vehicle injection (Fig. 4 *K* and *L* and *SI Appendix*, Fig. S7*B*). Thus, corticosterone not only causes persistent increases in AgRP neuron firing in ex

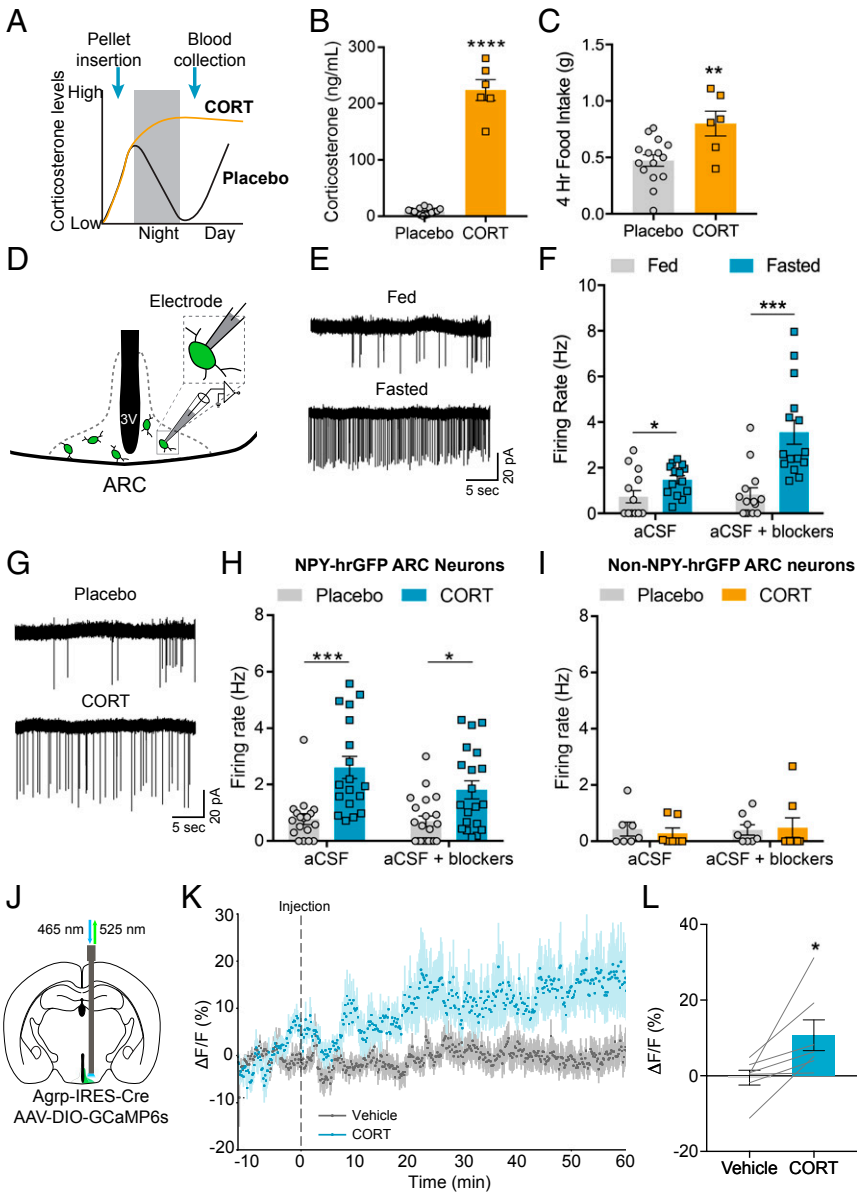

Fig. 4. Corticosterone increases the activity of AgRP neurons. (*A*) Experimental design of slow-release corticosterone pellet studies. Pellets were inserted at 16:00 with food weighed at 6:00, 8:00, and 10:00 the following day. At 10:00, blood was collected. (*B*) Plasma corticosterone levels of mice implanted with corticosterone pellets assessed 4 h after light-cycle onset (Placebo: $n = 15$; CORT: $n = 6$). Two-tailed unpaired t test. ****$P < 0.0001$. (*C*) Cumulative food intake of mice implanted with corticosterone pellets over the first 4 h of the light cycle (Placebo: $n = 15$; CORT: $n = 6$). Two-tailed unpaired t test. *$P < 0.01$. (*D*) Scheme of ex vivo cell-attached recordings from identified AgRP neurons. (*E*) Representative cell-attached recordings of AgRP neurons labeled by NPY-hrGFP from ad libitum-fed mice (*Top*) compared with 16-h–fasted mice (*Bottom*) in the presence of synaptic blockers. (*F*) Summary of NPY-hrGFP neuron firing rates from ad libitum-fed and 16-h–fasted mice (Fed-aCSF, $n = 14$ cells; Fed-aCSF+blockers, $n = 14$ cells; Fasted-aCSF, $n = 14$ cells; Fasted-aCSF+blockers, $n = 15$ cells from 3 fed and 3 fasted mice). Two-tailed unpaired t tests with Holm–Sidak multiple-comparisons correction. *$P < 0.05$; ***$P < 0.001$. (*G*) Representative cell-attached recordings of AgRP neurons labeled by NPY-hrGFP from mice implanted with a placebo pellet (*Top*) or a corticosterone pellet (*Bottom*) in the presence of synaptic blockers. (*H*) Summary of NPY-hrGFP–positive neuron firing rates from mice implanted with placebo or corticosterone pellets (Placebo-aCSF, $n = 18$ cells; Placebo-aCSF+blockers, $n = 21$ cells; CORT-aCSF, $n = 18$ cells; CORT-aCSF+blockers, $n = 20$ cells from 3 Placebo-implanted and 3 CORT-implanted mice). Two-tailed unpaired t tests with Holm–Sidak multiple-comparisons correction. *$P < 0.05$; ***$P < 0.001$. (*I*) Summary of NPY-hrGFP–negative neuron firing rates from mice implanted with placebo or corticosterone pellets (Placebo-aCSF, $n = 7$ cells; Placebo-aCSF+blockers, $n = 8$ cells; CORT-aCSF, $n = 7$ cells; CORT-aCSF+blockers, $n = 8$ cells from 2 Placebo-implanted and 2 CORT-implanted mice). (*J*) Schematic of fiber photometry from AgRP neurons expressing AAV-DIO-GCaMP6s. (*K*) Average calcium signal from AgRP neurons concurrent with s.c. injection of vehicle (gray) or corticosterone (2 mg/kg) (blue) ($n = 7$ mice; 2 trials per condition). (*L*) Average calcium responses of AgRP neurons following s.c. injection of vehicle or corticosterone ($n = 7$ mice; 2 trials per condition). Two-tailed paired t test. *$P < 0.05$. Data are the mean ± SEM.

vivo brain slices but also increases the activity of AgRP neurons in vivo.

Finally, because corticosterone has many targets within the brain and may activate AgRP neurons through modulation of their neural afferents, we sought to determine whether direct action of corticosterone on AgRP neurons was necessary to augment their activity. To do so, we overexpressed the glucocorticoid-inactivating enzyme 11β-hydroxysteroid dehydrogenase 2 (11β-HSD2) in AgRP neurons. 11β-HSD2 is a key regulator of active glucocorticoid levels as it converts corticosterone to its biologically inert isoform, dehydroxycorticosterone, thus preventing GR-mediated effects on gene expression (47–49). To visualize AgRP neurons in ex vivo brain slices, *Agrp*-IRES-Cre mice were crossed to L10-GFP Cre-reporter mice (50) (*Agrp*-IRES-Cre::L10-GFP mice). *Agrp*-IRES-Cre::L10-GFP mice were injected unilaterally with a Cre-dependent adeno-associated virus (AAV) driving the expression of mCherry-tagged 11β-HSD2 into the arcuate nucleus (Fig. 5*A*). Expression of 11β-HSD2 was confirmed to be specific to AgRP neurons (Fig. 5B). Subsequently, we recorded from AgRP neurons with (mCherry$^+$, GFP$^+$) or without (mCherry$^-$, GFP$^+$) 11β-HSD2 expression after fasting or corticosterone pellet treatment. Indeed, 11β-HSD2 overexpression in AgRP neurons blunted both the fasting-induced (Fig. 5 *C* and *D*) and corticosterone-mediated increase in AgRP neuron firing rate (Fig. 5 *E* and F). Together, these data suggest that corticosterone promotes appetite by directly increasing the firing of orexigenic AgRP neurons.

Corticosterone Promotes Fasting- and Hypoglycemia-Induced Hyperphagia through AgRP Neurons. To examine whether corticosterone signaling in AgRP neurons is necessary for the hyperphagia caused by elevated corticosterone, we bilaterally injected Cre-dependent AAV-*Hsd11b2*-2a-mCherry into the arcuate of *Agrp-IRES-Cre* mice. 11β-HSD2 overexpression in AgRP neurons completely abolished the hyperphagic effect of corticosterone pellets during the early light cycle (Fig. 6 *A* and *B*). Given that our work in rats demonstrated that corticosterone drives fasting and hypoglycemia-induced hyperphagia, we assessed whether food intake under these conditions is mediated by action of corticosterone on AgRP neurons. Indeed, expression of 11β-HSD2 in AgRP neurons significantly reduced food consumption following a fast (Fig. 6 *C* and *D*), while hypoglycemia-induced feeding was entirely abolished by 11β-HSD2 expression in AgRP neurons (Fig. 6 *E* and *F*). Furthermore,

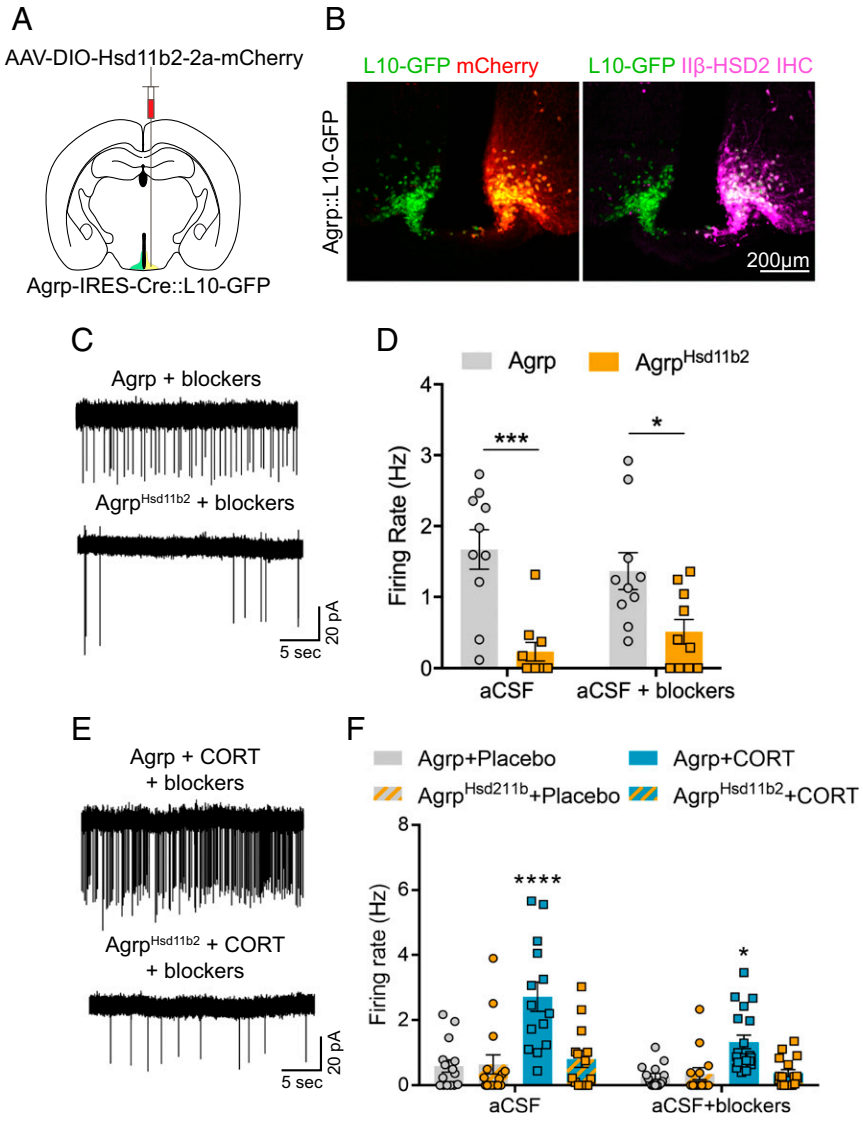

Fig. 5. Expression of 11β-HSD2 in AgRP neurons prevents corticosterone-mediated increases in their firing rate. (*A*) Schematic of unilateral AAV-DIO-Hsd11b2-2a-mCherry injections into AgRP-Cre neurons in *Agrp*-IRES-Cre::L10-GFP mice. (*B*) Representative unilateral 11β-HSD2-mCherry expression (*Left*) and 11β-HSD2 immunohistochemical staining (*Right*) from an *Agrp*-IRES-Cre::L10-GFP mouse. (*C*) Representative cell-attached recordings of Agrp::L10-GFP (*Top*) and Agrp::L10-GFP^{Hsd11b2} neurons (*Bottom*) from mice fasted for 16 h. (*D*) Summary of Agrp:L10-GFP and Agrp::L10-GFP^{Hsd11b2} neuron firing rates from mice fasted for 16 h (Agrp-aCSF, n = 10 cells; Agrp-aCSF+blockers, n = 10 cells; Agrp^{Hsd11b2}-aCSF, n = 10 cells; Agrp^{Hsd11b2}-aCSF+blockers, n = 10 cells from 3 fasted and 3 fed mice). Two-tailed unpaired t tests with Holm–Sidak multiple-comparisons correction. *P < 0.05; ***P < 0.001. (*E*) Representative cell-attached recordings of Agrp::L10-GFP (*Top*) and Agrp::L10-GFP^{Hsd11b2} neurons (*Bottom*) from mice implanted with corticosterone pellets. (*F*) Summary of Agrp::L10-GFP and AgRP::L10-GFP^{Hsd11b2} neuron firing rates from mice implanted with placebo or corticosterone pellets (Placebo Agrp-aCSF, n = 15 cells; Placebo Agrp^{Hsd11b2}-aCSF, n = 15 cells; CORT Agrp-aCSF, n = 14 cells; CORT AgRP^{Hsd11b2}-aCSF, n = 14 cells; Placebo Agrp-aCSF+blockers, n = 15 cells; Placebo Agrp^{Hsd11b2}-aCSF+blockers, n = 14 cells; CORT Agrp-aCSF+blockers, n = 19 cells; CORT AgRP^{Hsd11b2}-aCSF+blockers, n = 17 cells from 3 placebo-implanted and 3 CORT-implanted mice). Two-way ANOVA with Tukey's multiple-comparisons test. *P < 0.05; ****P < 0.0001. Data are the mean ± SEM.

11β-HSD2–expressing mice ate less during the early dark cycle when corticosterone is at its daily peak (*SI Appendix*, Fig. S7 *C* and *D*), and 24-h food intake was also reduced (*SI Appendix*, Fig. S7*E*). These data demonstrate that corticosterone's effects on food intake under multiple conditions is mediated by its action on AgRP neurons and that this mechanism is entirely responsible for hypoglycemia-induced food intake.

Discussion

Despite their differing etiologies, hypoglycemia (51–59), poorly controlled diabetes (17, 55, 60–69), and starvation (70–74) are all well-known triggers of hyperphagia. Our current study demonstrates that hyperphagia driven by these states is dependent upon hypercorticosteronemia and that the effect of leptin to reduce food intake in starvation and poorly controlled diabetes is mediated through suppression of the HPA axis. Furthermore, we show that activation of appetite-promoting AgRP neurons in the hypothalamic arcuate nucleus by corticosterone underlies these effects. While surprising, these results are in line with prior work linking elevated corticosterone to hyperphagia, weight gain, and increased expression of the orexigenic neuropeptides NPY and AgRP in the arcuate (22–24, 75). Furthermore, most prior studies (76–81), but not all (82), have found that adrenalectomy moderates the development of obesity in leptin-deficient rodents; however, these studies attributed the finding that adrenalectomy reduced food intake in leptin-deficient rodents to multiple alternative mechanisms and did not implicate stimulation of AgRP neuron firing by glucocorticoids.

It is generally believed that leptin does not regulate the HPA axis in humans because some leptin-deficient humans, unlike leptin-deficient rodents, do not have elevated glucocorticoids (83, 84). However, evidence to the contrary exists: Patients with congential leptin deficiency (85, 86) or endocrine dysfunction concomitant with hypoleptinemia (87) present with elevated cortisol, which can be rescued with leptin treatment (87). Furthermore, humans with low glucocorticoids have reduced hunger and body weight (88, 89), and increased cortisol stimulates appetite in humans (90, 91). Our current findings and the discrepancies regarding HPA axis regulation of hyperphagia in humans with leptin deficiency strongly suggest that further examination of this system is warranted.

The hyperphagia that occurs in response to glucose deprivation is also dependent upon hypercorticosteronemia, but independent of leptin deficiency, in contrast to fasting and T1D. This suggests a different mechanism for HPA axis activation during hypoglycemia. Indeed, C1 catecholaminergic neurons in the

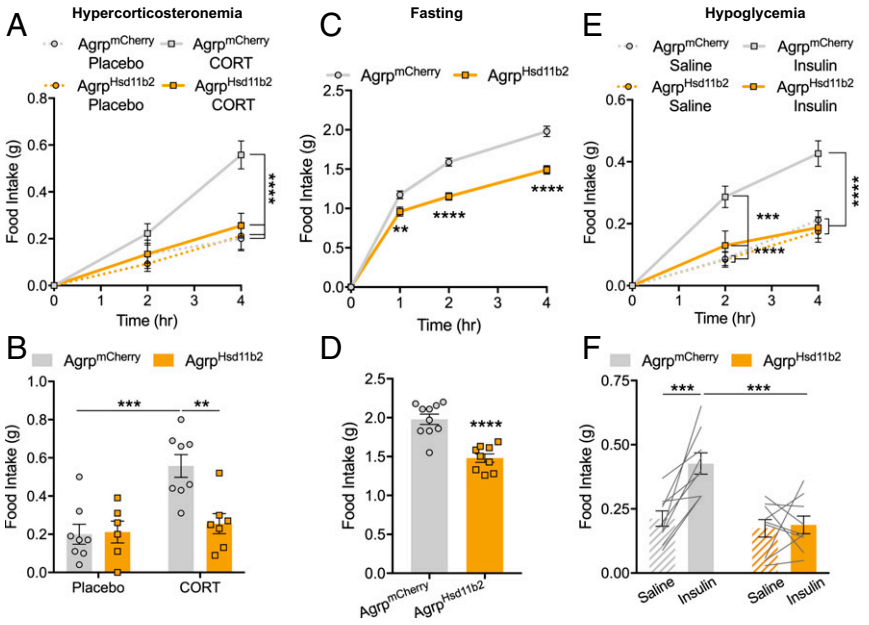

Fig. 6. Hypercorticosteronemia-induced food intake is mediated by AgRP neurons. (*A*) Time course of food intake of Agrp^{mCherry} and Agrp$^{Hsd11\beta2}$ mice implanted with placebo or corticosterone pellets (n = 6–8 per group). Two-way repeated-measures ANOVA with Tukey's multiple-comparisons test. ****P < 0.0001. (*B*) Four-hour cumulative food intake of Agrp^{mCherry} and Agrp$^{Hsd11\beta2}$ mice implanted with placebo or corticosterone pellets (n = 6–8 per group). Two-way ANOVA with Tukey's multiple-comparisons test. ***P < 0.001; **P < 0.01. (*C*) Time course of postfast food intake of Agrp^{mCherry} and Agrp$^{Hsd11\beta2}$ mice (Agrp^{mCherry}, n = 10; Agrp$^{Hsd11\beta2}$, n = 9). Two-way repeated-measures ANOVA with Tukey's multiple-comparisons test. **P < 0.01, ****P < 0.0001. (*D*) Four-hour cumulative postfast food intake of Agrp^{mCherry} and Agrp$^{Hsd11\beta2}$ mice (Agrp^{mCherry}, n = 10; Agrp$^{Hsd11\beta2}$, n = 9). Two-tailed unpaired t test. ****P < 0.0001. (*E*) Time course of hypoglycemia-induced food intake of Agrp^{mCherry} and Agrp$^{Hsd11\beta2}$ mice (Agrp^{mCherry}, n = 9; Agrp$^{Hsd11\beta2}$, n = 9). Two-way ANOVA with Tukey's multiple-comparisons test. ***P < 0.001; ****P < 0.0001. (*F*) Four-hour cumulative hypoglycemia-induced food intake of Agrp^{mCherry} and Agrp$^{Hsd11\beta2}$ mice (Agrp^{mCherry}, n = 9; Agrp$^{Hsd11\beta2}$, n = 9). Two-way ANOVA with Tukey's multiple-comparisons test. ***P < 0.001. Data are the mean ± SEM.

ventrolateral medulla, which are activated by hypoglycemia and are viewed as playing a key role in transducing the vital counterregulatory responses (92), stimulate both glucocorticoids and feeding (34). This is likely mediated through their projections to the paraventricular nucleus of the hypothalamus, suggesting that these neurons directly regulate the HPA axis (34, 92). Previously, insulin or 2-deoxyglucose–induced glucoprivation was shown to increase *Agrp* and *Npy* transcripts in the arcuate (93, 94), suggesting that AgRP neurons are likely involved in driving the hypoglycemia-induced hyperphagia. Strikingly, 11β-HSD2 expression in AgRP neurons blocked hypoglycemia-induced hyperphagia (93, 94), indicating that hypoglycemic activation of the HPA axis and subsequent corticosterone-mediated stimulation of AgRP neurons is necessary for the induction of hypoglycemia-driven feeding.

Inhibition of glucocorticoid signaling in AgRP neurons blocked hyperphagia induced by hypercorticosteronemia and hypoglycemia, while prominently reducing food intake after fasting. However, the molecular mechanism underlying corticosterone activation of AgRP neurons is unknown. Glucocorticoids primarily regulate gene expression, but the genomic effects of corticosterone signaling are dependent upon many factors, including cell type, and are not fully characterized (95). Given that AgRP neuron action potential firing caused by fasting or hypercorticosteronemia persists ex vivo in the presence of synaptic blockers, corticosterone signaling may drive expression of genes that promote cell-autonomous activity. We have previously proposed similar actions by aldosterone on neurons that drive sodium appetite in the hindbrain (96). In addition, nongenomic effects of corticosterone signaling, which are often mediated through modulation of synaptic inputs (97), may contribute to driving AgRP neuron activity. Indeed, excitatory inputs to AgRP neurons are strengthened during fasting (15, 42), and corticosterone was previously reported to regulate synaptic input organization and excitability of AgRP neurons (98). Our findings that corticosterone signaling in AgRP neurons is necessary for hyperphagia contrast with a previous report that mice lacking glucocorticoid receptors specifically in AgRP neurons show little to no reduction in food intake or body weight (99). However, compensatory actions of mineralocorticoid receptors, which bind corticosterone with high affinity, may account for these findings. In addition, compensation for AgRP neuron loss of function has been reported in other studies including neonatal ablation (100, 101) and developmental deletion of leptin receptors (17, 102). Future studies leveraging RNA-sequencing technology to examine gene targets and recordings of AgRP neuron activity in the presence and absence of corticosterone signaling are needed to decipher which genomic and nongenomic mechanisms are involved in hypercorticosteronemia-mediated stimulation of AgRP neurons.

In summary, these findings reveal that hunger driven by hypoleptinemia or hypoglycemia is not entirely mediated via CNS circuits. Unexpectedly, both hypoleptinemia and hypoglycemia recruit and require an HPA axis–AgRP neuron pathway to fully induce hunger. We further demonstrate that the majority of leptin-mediated suppression of hyperphagia occurs through its ability to suppress hypercorticosteronemia in the transition from low to physiologic leptin concentrations (25, 26, 103). Finally, this study provides evidence for stimulation of a glucocorticoid–AgRP neuron axis that promotes food intake and suggests that AgRP neurons may be an attractive therapeutic target to suppress hyperphagia under conditions of leptin deficiency or glucocorticoid excess including Cushing's disease.

Methods

Animals. All protocols were approved by the Institutional Animal Care and Use Committees of Yale University or Beth Israel Deaconess Medical Center. In the rat studies, healthy male rats weighing 250–300 g were ordered from Charles River Laboratories and maintained on regular chow (Harlan Teklad; 2018). Where indicated, adrenalectomy was performed by Charles River, and ADX rats were maintained on drinking water containing 0.9% NaCl and 2%

sucrose. Upon arrival, they were housed in a 12-h light/dark cycle at ∼25 °C, and underwent surgery under isoflurane anesthesia to place catheters in the jugular vein and common carotid artery as well as an Alzet pump to deliver low-dose (7.5 mg/d) or high-dose (20 mg/d) corticosterone. Arterial catheters were used for all rat infusions, while venous catheters were used for blood sampling. To avoid any effects of diurnal variation on food intake, all acute food intake measurements were obtained between 2:00 and 4:00 PM following the fasting times listed in the figure legends. At 10:00 AM, treatment with leptin, corticosterone, and/or mifepristone, as described below, was begun following 42 h of food withdrawal or at the time of food withdrawal as designated in the figure legends (final fasting time, 6 or 48 h). ADX rats were given access to NaCl/sucrose-containing water throughout the fast, but food was removed 48 h before the study. After a fast–refeeding study, ADX rats were placed on HFD (Research Diets; 12492) for 2 wk, after which the fast–refeeding study was repeated. In all rat studies, food intake was measured by a blinded investigator, who weighed food before and after refeeding.

To induce poorly controlled T1D, rats were injected with 65 mg/kg streptozotocin after an overnight fast at 9:00 AM the morning before the study, and then refed. At 7:00 PM, food was removed. Plasma insulin concentrations were measured after a 15-h fast, and those with plasma glucose concentrations <160 mg/dL were later removed from analysis. Beginning at 10:00 AM, they were treated with leptin, corticosterone, and/or mifepristone as described below. Food was provided at 2:00 PM, and rats were allowed to eat ad libitum until they were killed at 4:00 PM.

Four-hour euglycemic and hypoglycemic clamps were performed beginning at 10:00 AM after an overnight fast. In both cases, insulin was infused intraarterially (prime 40 mU/kg, continuous infusion 4 mU/[kg·min]), and a variable infusion of 20% dextrose was administered to maintain euglycemia (∼120 mg/dL) or hypoglycemia (∼60 mg/dL). After 4 h, food was provided ad libitum and the insulin and glucose infusions were continued, but the infusion rates were not adjusted for the remaining 2 h of the study.

Before the VLCD study, rats were fed HFD for 4 wk, and plasma hormones and food intake were measured following a 48-h fast. They were then placed on a VLCD (2 g diet per day, ∼25% of their usual intake) for 4 wk, thereby returning their body weights to the typical healthy range. The fasting study was repeated, with hormones measured a second time.

Sham-operated and ADX male mice were obtained from The Jackson Laboratory at 8 wk of age. Upon arrival, they underwent surgery to place Alzet pumps to deliver low (0.75 mg/d) or high dose (2.0 mg/d) corticosterone. Mice were maintained on 0.9% NaCl/2% sucrose water throughout the study. Body composition analysis was performed by NMR spectroscopy using the Bruker Minispec, and energetics, food and water consumption, and activity were monitored for 3 d using Columbus Instruments' Comprehensive Lab Animal Monitoring System. Mice were fasted for 24 h (with access to 0.9% NaCl/2% sucrose water) or fed ad libitum as indicated in the figures. After a metabolic cage study, they were placed on a lard-based HFD (Dyets; 112245; 60% calories from fat) for 2 wk, after which the metabolic cage studies were repeated. To avoid any confounding effects of different diet palatability, mice were refed regular chow after the 2-wk high-fat feeding period.

Wild-type mice (C57BL/6J) for corticosterone pellet studies were obtained from The Jackson Laboratory and singly housed before experiments. For experiments targeting AgRP neurons, mice aged 8–12 wk were used. The mice were singly housed in a temperature- and humidity-controlled room with a 12-h light/dark cycle before experiments. Mice had ad libitum access to standard chow (Envigo Teklad F6 8664) and water. *Agrp-IRES-Cre* (45), *Agrp-IRES-Cre*::lox-L10-GFP (50), and *Npy-hrGFP* (44) mice were maintained on a mixed background. For behavioral and electrophysiological studies, male mice were used. For corticosterone pellet studies, mice were implanted with slow-release corticosterone pellets (Innovative Research of America) under isoflurane anesthesia. Pellets were placed in the lateral skin of the neck 2 h before dark-cycle onset. The following day, food in the home cage was weighed at the onset of the light cycle and after 2 and 4 h. The mice were then rapidly decapitated, and trunk blood was collected for hormone measurements. Fasting-induced food intake was performed after a 16-h fast (from 2 h before lights offset to 2 h after light onset). Preweighed food was provided for a total of 4 h, with intake being weighed after 1, 2, and 4 h. Hypoglycemia-induced feeding studies were conducted in the early light cycle. Singly housed mice were intraperitoneally injected with insulin (Lilly) (10 μL/g) at 2 units/kg body weight 3 h after onset of the light cycle. Food intake was measured at the beginning of the experiment and after 2 and 4 h.

Leptin, Corticosterone, and Mifepristone Treatment. Where indicated, rats were infused intraarterially with leptin (60 pmol/[kg·min]) and/or corticosterone (187.5 μg/kg) over 6 h, beginning at 10:00 AM and continuing through the refeeding period. Rats treated with mifepristone were given an i.p. injection of the drug (10 mg/kg) solubilized in 10% ethanol/90% normal saline at 12:00 PM, 2 h before refeeding.

Stereotaxic AAV Injections. pAAV-hSyn-DIO-HSD11b2-t2a-mCherry was constructed by inserting the HSD11b2-t2a-mCherry in reverse orientation in between 2 sets of opposite lox sites and downstream of the human synapsin promoter. AAV production was done by the Boston Children's Hospital Viral Core. For injections into the arcuate nucleus, mice were anesthetized with xylazine (5 mg per kg) and ketamine (75 mg per kg) diluted in saline (350 mg/kg), and placed into a stereotaxic apparatus (KOPF; model 963). For postoperative care, mice were injected s.c. with sustained release meloxicam (4 mg/kg). After exposing the skull via a small incision, a small hole was drilled for injection. A pulled-glass pipette with a 20- to 40-μm tip diameter was inserted into the brain and virus was injected by an air pressure system. A micromanipulator (Grass Technologies; model S48 stimulator) was used deliver the injection at 25 nL·min^{-1} and the pipette was withdrawn 5 min after injection. For behavior experiments AAV8-hSyn-DIO-mCherry (UNC Vector Core) or AAV8-hSyn-DIO-*Hsd11b2*-t2a-mCherry was injected into *Agrp*-IRES-Cre mice at 6 sites to cover the anterior-posterior extent of the arcuate (50 nL per site; bregma: anteroposterior [AP], −1.30 and −1.45 mm; dorsoventral [DV], −5.85 mm; mediolateral [ML], −0.3 , 0 , +0.3 mm). For electrophysiology studies, AAV-DIO-*Hsd11b2*-t2a-mCherry was injected unilaterally into Agrp-IRES-Cre::L10-GFP mice (50 nL; bregma: AP, −1.4 mm; DV, −5.85; ML, −0.35 mm). For fiber photometry experiments, AAV1-hSyn-DIO-GCaMP6s (University of Pennsylvania Vector Core) was injected into the arcuate of Agrp-IRES-Cre mice. Animals were allowed to recover from stereotaxic surgery a minimum of 14 d before experiments. Following each experimental procedure, the accuracy of AAV injections was confirmed via post hoc histological analysis of XFP reporters. All subjects determined to be surgical "misses" based on little or absent reporter expression were removed from analyses.

Optic Fiber Implantation. For fiber photometry recordings, an optic fiber was implanted in the same surgery as virus injection. A metal ferrule optic fiber (400-μm-diameter core; BFH37-400 Multimode; NA 0.48; Thor Labs) was implanted unilaterally over the arcuate (AP, −1.45 mm; DV, −5.8 mm; ML, −0.25 mm from bregma). Fibers were fixed to the skull using dental acrylic. Following experiments and histology of the brain tissue, the location of the fiber tips was identified.

In Vivo Fiber Photometry Recordings. Fiber photometry was performed on a rig constructed as follows: A 465-nm LED (PlexBright LED Module and LD-1 Driver; Plexon) was used as the excitation source, which was passed through a fluorescence mini cube (excitation, 460–490 nm; detection, 500–550 nm; Doric Lenses) and transmitted onto the sample via a fiber optic cable (1 m long; 400 μm diameter; N.A., 0.48; Doric Lenses). The optic fiber was coupled to the implanted optic fiber with a ceramic mating sleeve (Thor Labs). Light intensity was measured as 0.2–0.3 mW at the end of the patch cord and was kept constant across sessions for each mouse. Emitted light was collected by a photodetector (2151; Newport). The signal was digitized at 1 kHz with a National Instruments data acquisition card and collecting with a custom MATLAB (MATLAB 2016a; MathWorks) script. To reduce photobleaching during 1-h-long recordings, the LED was pulsed for 1 s every 10 s by a pulse generator (Arduino) as in ref. 46.

Recordings were performed within-subject, with animals receiving 2 vehicle [10% polyethylene glycol 400 (Millipore) in saline] and 2 corticosterone (Sigma) trials (2 mg/kg in vehicle). The trial order was counterbalanced with 1 rest day between each recording session. Mice were habituated to s.c. injections and tethering to the optic fiber cable for 2 d before the first day of recording. Recordings were performed in the home cage early in the light cycle with food removed from the cage during the recordings.

Data were analyzed using a custom Python (Python 3.6) script. The median fluorescence value of each LED pulse was taken to condense each pulse into a single data point. The average fluorescence change was calculated as $\Delta F/F = (F - F0)/F0$, where F0 was the mean of all data points from the 15-min baseline before injection, for each recording session.

Biochemical Analysis. Plasma glucose was measured using the YSI Glucose Analyzer. Plasma insulin, leptin, corticosterone, and ACTH concentrations were measured by ELISA (Mercodia, R&D Systems, Alpco, and MyBioSource, respectively), with the exception of the hypoglycemic clamps in which insulin concentrations were measured by radioimmunoassay by the Yale Diabetes Research Core. To assess corticosterone levels in mice implanted with

slow-release pellets, trunk blood was taken following sacrifice and centrifuged for plasma collection. Plasma was run in duplicate in a 96-well plate ELISA kit for corticosterone (Enzo Life Sciences) according to the manufacturer's protocol.

Electrophysiology Studies. Loose-seal, cell-attached recordings were performed as described previously with minor modifications (96). Briefly, brains were quickly removed and placed into ice-cold cutting solution consisting of the following (in mM): 92 choline chloride, 10 Hepes, 2.5 KCl, 1.25 NaH_2PO4, 30 $NaHCO_3$, 25 glucose, 10 $MgSO_4$, 0.5 $CaCl_2$, 2 thiourea, 5 sodium ascorbate, 3 sodium pyruvate, oxygenated with 95% O_2/5% CO_2, with measured osmolarity of 310–320 mOsm/L, and pH 7.4. The 200- to 300-μm-thick coronal sections containing the arcuate were cut with a vibratome and incubated in oxygenated cutting solution at 34 °C for 10 min. Slices were transferred to oxygenated aCSF (126 mM NaCl, 21.4 mM $NaHCO_3$, 2.5 mM KCl, 1.2 mM NaH_2PO_4, 1.2 mM $MgCl_2$, 2.4 mM $CaCl_2$, 10 mM glucose) at 34 °C for 15 min and then stored in the same solution at room temperature (20–24 °C) for at least 60 min before recording. Loose-seal, cell-attached recordings (seal resistance, 20–50 MΩ) were made in voltage-clamp mode with aCSF as internal solution and holding current maintained at $V_h = 0$ mV. Where indicated, synaptic blockers [including kynurenate (1 mM) and picrotoxin (100 μm)] were included in the bath solution to synaptically isolate AgRP neurons. All recordings were made using a Multiclamp 700B amplifier, and data were filtered at 2 kHz and digitized at 10 or 20 kHz before analysis off-line using Clampfit 10.

Histology. Immunofluorescence was performed as described previously (96). Briefly, mice were terminally anesthetized with 7% choral hydrate (500 mg·kg^{-1}; Sigma-Aldrich) diluted in saline and transcardially perfused with 0.1 M PBS followed by 10% neutral-buffered formalin solution (NBF) (Thermo Fisher Scientific). Brains were extracted and postfixed overnight at 4 °C in NBF, cryoprotected in 20% sucrose, and sectioned coronally at 30 μm on a freezing microtome (Leica Biosystems). The following primary antibodies were used overnight at room temperature: rabbit anti-HSD2 (H-145; Santa Cruz Biotechnology), 1:300; rat anti-mCherry (Life Technologies), 1:3,000. The following day, the sections were washed and incubated at room temperature in donkey Alexa Fluor fluorescent secondary antibody (Life Technologies; 1:1,000). Fluorescent images were captured using an Olympus VS120 slide-scanning microscope.

Data Analysis. Statistical analyses were performed using Prism 7 (GraphPad) software and are described in the figure legends. No statistical method was used to predetermine sample size, nor were randomization and blinding methods used, and statistical significance was defined as $P < 0.05$. All data presented met the assumptions of the statistical test employed. Experimental animals were excluded if histological validation revealed poor or absent reporter expression. *N* values reflect the final number of validated animals per group.

ACKNOWLEDGMENTS. We thank J. Dong, W. Zhu, A. Nasiri, Y. Li, J. Berrios, Z. Yang, and J. Yu for their invaluable technical contributions. This study was funded by grants from the US Public Health Service (R01 DK-113984, P30 DK-059635, T32 DK-101019, K99/R00 CA-215315, R01 NS-087568, UL1TR000142, T32 DK-007058, R01 DK-075632, R01 DK-089044, R01 DK-096010, R01 DK-111401, K99/R00 HL-144923, P30 DK-046200, and P30 DK-057521) as well as an investigator-initiated award from AstraZeneca and a fellowship from Naomi Berrie Diabetes Center.

1. Y. Zhang *et al*., Positional cloning of the mouse obese gene and its human homologue. *Nature* **372**, 425–432 (1994).
2. L. A. Campfield, F. J. Smith, Y. Guisez, R. Devos, P. Burn, Recombinant mouse OB protein: Evidence for a peripheral signal linking adiposity and central neural networks. *Science* **269**, 546–549 (1995).
3. M. A. Pelleymounter *et al*., Effects of the obese gene product on body weight regulation in *ob/ob* mice. *Science* **269**, 540–543 (1995).
4. J. L. Halaas *et al*., Weight-reducing effects of the plasma protein encoded by the obese gene. *Science* **269**, 543–546 (1995).
5. S. B. Heymsfield *et al*., Recombinant leptin for weight loss in obese and lean adults: A randomized, controlled, dose-escalation trial. *JAMA* **282**, 1568–1575 (1999).
6. B. Mittendorfer *et al*., Recombinant human leptin treatment does not improve insulin action in obese subjects with type 2 diabetes. *Diabetes* **60**, 1474–1477 (2011).
7. M. Van Heek *et al*., Diet-induced obese mice develop peripheral, but not central, resistance to leptin. *J. Clin. Invest.* **99**, 385–390 (1997).
8. I. S. Farooqi *et al*., Effects of recombinant leptin therapy in a child with congenital leptin deficiency. *N. Engl. J. Med.* **341**, 879–884 (1999).
9. K. F. Petersen *et al*., Leptin reverses insulin resistance and hepatic steatosis in patients with severe lipodystrophy. *J. Clin. Invest.* **109**, 1345–1350 (2002).
10. J. R. McDuffie *et al*., Effects of exogenous leptin on satiety and satiation in patients with lipodystrophy and leptin insufficiency. *J. Clin. Endocrinol. Metab.* **89**, 4258–4263 (2004).
11. J. Licinio *et al*., Phenotypic effects of leptin replacement on morbid obesity, diabetes mellitus, hypogonadism, and behavior in leptin-deficient adults. *Proc. Natl. Acad. Sci. U.S.A.* **101**, 4531–4536 (2004).
12. A. De Paoli, A. Long, G. M. Fine, M. Stewart, S. O'Rahilly, Efficacy of metreleptin for weight loss in overweight and obese adults with low leptin levels. *Diabetes* **67** (suppl. 1), LB77 (2018).
13. M. Wabitsch *et al*., Biologically inactive leptin and early-onset extreme obesity. *N. Engl. J. Med.* **372**, 48–54 (2015).
14. L. E. Ring, L. M. Zeltser, Disruption of hypothalamic leptin signaling in mice leads to early-onset obesity, but physiological adaptations in mature animals stabilize adiposity levels. *J. Clin. Invest.* **120**, 2931–2941 (2010).
15. L. Vong *et al*., Leptin action on GABAergic neurons prevents obesity and reduces inhibitory tone to POMC neurons. *Neuron* **71**, 142–154 (2011).
16. R. L. Leshan, M. Greenwald-Yarnell, C. M. Patterson, I. E. Gonzalez, M. G. Myers, Jr, Leptin action through hypothalamic nitric oxide synthase-1-expressing neurons controls energy balance. *Nat. Med.* **18**, 820–823 (2012).
17. J. Xu *et al*., Genetic identification of leptin neural circuits in energy and glucose homeostases. *Nature* **556**, 505–509 (2018).
18. Y. Aponte, D. Atasoy, S. M. Sternson, AGRP neurons are sufficient to orchestrate feeding behavior rapidly and without training. *Nat. Neurosci.* **14**, 351–355 (2011).
19. M. J. Krashes *et al*., Rapid, reversible activation of AgRP neurons drives feeding behavior in mice. *J. Clin. Invest.* **121**, 1424–1428 (2011).
20. S. Hisano *et al*., Localization of glucocorticoid receptor in neuropeptide Y-containing neurons in the arcuate nucleus of the rat hypothalamus. *Neurosci. Lett.* **95**, 13–18 (1988).
21. J. N. Campbell *et al*., A molecular census of arcuate hypothalamus and median eminence cell types. *Nat. Neurosci.* **20**, 484–496 (2017).
22. A. Akabayashi *et al*., Hypothalamic neuropeptide Y, its gene expression and receptor activity: Relation to circulating corticosterone in adrenalectomized rats. *Brain Res.* **665**, 201–212 (1994).
23. X. Y. Lu *et al*., Diurnal rhythm of agouti-related protein and its relation to corticosterone and food intake. *Endocrinology* **143**, 3905–3915 (2002).
24. P. Ponsalle, L. S. Srivastava, R. M. Uht, J. D. White, Glucocorticoids are required for food deprivation-induced increases in hypothalamic neuropeptide Y expression. *J. Neuroendocrinol.* **4**, 585–591 (1992).
25. R. J. Perry *et al*., Mechanism for leptin's acute insulin-independent effect to reverse diabetic ketoacidosis. *J. Clin. Invest.* **127**, 657–669 (2017).
26. R. J. Perry *et al*., Leptin reverses diabetes by suppression of the hypothalamic-pituitary-adrenal axis. *Nat. Med.* **20**, 759–763 (2014).
27. X. Yu, B. H. Park, M. Y. Wang, Z. V. Wang, R. H. Unger, Making insulin-deficient type 1 diabetic rodents thrive without insulin. *Proc. Natl. Acad. Sci. U.S.A.* **105**, 14070–14075 (2008).
28. T. Fujikawa, J. C. Chuang, I. Sakata, G. Ramadori, R. Coppari, Leptin therapy improves insulin-deficient type 1 diabetes by CNS-dependent mechanisms in mice. *Proc. Natl. Acad. Sci. U.S.A.* **107**, 17391–17396 (2010).
29. R. Gomez *et al*., Acute intraperitoneal administration of taurine decreases the glycemia and reduces food intake in type 1 diabetic rats. *Biomed. Pharmacother.* **103**, 1028–1034 (2018).
30. E. H. Hathout *et al*., Changes in plasma leptin during the treatment of diabetic ketoacidosis. *J. Clin. Endocrinol. Metab.* **84**, 4545–4548 (1999).
31. A. E. Kitabchi, G. E. Umpierrez, Changes in serum leptin in lean and obese subjects with acute hyperglycemic crises. *J. Clin. Endocrinol. Metab.* **88**, 2593–2596 (2003).
32. H. C. Denroche *et al*., Leptin therapy reverses hyperglycemia in mice with streptozotocin-induced diabetes, independent of hepatic leptin signaling. *Diabetes* **60**, 1414–1423 (2011).
33. M. C. Amato *et al*., Relative hypoleptinemia in poorly controlled patients with type 1 diabetes. *Horm. Metab. Res.* **39**, 398–399 (2007).
34. S. Ritter, A. G. Watts, T. T. Dinh, G. Sanchez-Watts, C. Pedrow, Immunotoxin lesion of hypothalamically projecting norepinephrine and epinephrine neurons differentially affects circadian and stressor-stimulated corticosterone secretion. *Endocrinology* **144**, 1357–1367 (2003).
35. K. Abe, J. Kroning, M. A. Greer, V. Critchlow, Effects of destruction of the suprachiasmatic nuclei on the circadian rhythms in plasma corticosterone, body temperature, feeding and plasma thyrotropin. *Neuroendocrinology* **29**, 119–131 (1979).
36. R. S. Ahima *et al*., Role of leptin in the neuroendocrine response to fasting. *Nature* **382**, 250–252 (1996).
37. M. F. Dallman *et al*., Starvation: Early signals, sensors, and sequelae. *Endocrinology* **140**, 4015–4023 (1999).
38. F. Spiga, J. J. Walker, J. R. Terry, S. L. Lightman, HPA axis-rhythms. *Compr. Physiol.* **4**, 1273–1298 (2014).
39. M. J. Krashes, B. P. Shah, S. Koda, B. B. Lowell, Rapid versus delayed stimulation of feeding by the endogenously released AgRP neuron mediators GABA, NPY, and AgRP. *Cell Metab.* **18**, 588–595 (2013).
40. Y. Mandelblat-Cerf *et al*., Arcuate hypothalamic AgRP and putative POMC neurons show opposite changes in spiking across multiple timescales. *eLife* **4**, e07122 (2015).
41. K. A. Takahashi, R. D. Cone, Fasting induces a large, leptin-dependent increase in the intrinsic action potential frequency of orexigenic arcuate nucleus neuropeptide Y/Agouti-related protein neurons. *Endocrinology* **146**, 1043–1047 (2005).

42. T. Liu *et al*., Fasting activation of AgRP neurons requires NMDA receptors and involves spinogenesis and increased excitatory tone. *Neuron* **73**, 511–522 (2012).
43. Y. Yang, D. Atasoy, H. H. Su, S. M. Sternson, Hunger states switch a flip-flop memory circuit via a synaptic AMPK-dependent positive feedback loop. *Cell* **146**, 992–1003 (2011).
44. A. N. van den Pol *et al*., Neuromedin B and gastrin-releasing peptide excite arcuate nucleus neuropeptide Y neurons in a novel transgenic mouse expressing strong Renilla green fluorescent protein in NPY neurons. *J. Neurosci.* **29**, 4622–4639 (2009).
45. Q. Tong, C. P. Ye, J. E. Jones, J. K. Elmquist, B. B. Lowell, Synaptic release of GABA by AgRP neurons is required for normal regulation of energy balance. *Nat. Neurosci.* **11**, 998–1000 (2008).
46. L. R. Beutler LR *et al*., Dynamics of gut-brain communication underlying hunger. *Neuron* **96**, 461–475.e5 (2017).
47. C. Monder, C. H. Shackleton, 11β-Hydroxysteroid dehydrogenase: Fact or fancy? *Steroids* **44**, 383–417 (1984).
48. C. S. Wyrwoll, M. C. Holmes, J. R. Seckl, 11β-Hydroxysteroid dehydrogenases and the brain: From zero to hero, a decade of progress. *Front. Neuroendocrinol.* **32**, 265–286 (2011).
49. J. W. Funder, P. T. Pearce, R. Smith, A. I. Smith, Mineralocorticoid action: Target tissue specificity is enzyme, not receptor, mediated. *Science* **242**, 583–585 (1988).
50. M. J. Krashes *et al*., An excitatory paraventricular nucleus to AgRP neuron circuit that drives hunger. *Nature* **507**, 238–242 (2014).
51. K. P. Briski, T. P. Nedungadi, Adaptation of feeding and counter-regulatory hormone responses to intermediate insulin-induced hypoglycaemia in the ovariectomised female rat: Effects of oestradiol. *J. Neuroendocrinol.* **21**, 578–585 (2009).
52. T. P. Nedungadi, K. P. Briski, Effects of intracerebroventricular administration of the NPY-Y1 receptor antagonist, 1229U91, on hyperphagic and glycemic responses to acute and chronic intermediate insulin-induced hypoglycemia in female rats. *Regul. Pept.* **159**, 14–18 (2010).
53. E. Gallmann, D. Arsenijevic, M. Spengler, G. Williams, W. Langhans, Effect of CCK-8 on insulin-induced hyperphagia and hypothalamic orexigenic neuropeptide expression in the rat. *Peptides* **26**, 437–445 (2005).
54. X. J. Cai *et al*., Hypoglycemia activates orexin neurons and selectively increases hypothalamic orexin-B levels: Responses inhibited by feeding and possibly mediated by the nucleus of the solitary tract. *Diabetes* **50**, 105–112 (2001).
55. L. L. Bellush, S. G. Reid, Metabolic and neurochemical profiles in insulin-treated diabetic rats. *Am. J. Physiol.* **266**, R87–R94 (1994).
56. S. E. Corrin, H. D. McCarthy, P. E. McKibbin, G. Williams, Unchanged hypothalamic neuropeptide Y concentrations in hyperphagic, hypoglycemic rats: Evidence for specific metabolic regulation of hypothalamic NPY. *Peptides* **12**, 425–430 (1991).
57. P. R. Flatt, K. S. Tan, S. K. Swanston-Flatt, C. J. Bailey, V. Marks, Defective diurnal changes of food intake, plasma glucose and insulin in rats with a transplantable islet cell tumour. *Horm. Res.* **27**, 47–52 (1987).
58. D. DiBattista, Characteristics of insulin-induced hyperphagia in the golden hamster. *Physiol. Behav.* **32**, 381–387 (1984).
59. D. DiBattista, Food deprivation and insulin-induced feeding in the hamster. *Physiol. Behav.* **30**, 683–687 (1983).
60. P. R. Flatt, C. J. Bailey, J. M. Conlon, Somatostatin, gastrin-releasing peptide and gastrin in the stomach of rats with streptozotocin-induced diabetes and insulinoma. *J. Nutr.* **121**, 1414–1417 (1991).
61. Y. Xu, J. T. Chang, M. G. Myers, Jr, Y. Xu, Q. Tong, Euglycemia restoration by central leptin in type 1 diabetes requires STAT3 signaling but not fast-acting neurotransmitter release. *Diabetes* **65**, 1040–1049 (2016).
62. M. Naito *et al*., Therapeutic impact of leptin on diabetes, diabetic complications, and longevity in insulin-deficient diabetic mice. *Diabetes* **60**, 2265–2273 (2011).
63. K. Iwata *et al*., Involvement of brain ketone bodies and the noradrenergic pathway in diabetic hyperphagia in rats. *J. Physiol. Sci.* **61**, 103–113 (2011).
64. M. Toyoshima *et al*., Dimorphic gene expression patterns of anorexigenic and orexigenic peptides in hypothalamus account male and female hyperphagia in Akita type 1 diabetic mice. *Biochem. Biophys. Res. Commun.* **352**, 703–708 (2007).
65. D. K. Sindelar *et al*., Low plasma leptin levels contribute to diabetic hyperphagia in rats. *Diabetes* **48**, 1275–1280 (1999).
66. D. Rebolledo-Solleiro, A. Fernández-Guasti, Influence of sex and estrous cycle on blood glucose levels, body weight gain, and depressive-like behavior in streptozotocin-induced diabetic rats. *Physiol. Behav.* **194**, 560–567 (2018).
67. A. A. da Silva, J. N. Freeman, J. E. Hall, J. M. do Carmo, Control of appetite, blood glucose, and blood pressure during melanocortin-4 receptor activation in normoglycemic and diabetic NPY-deficient mice. *Am. J. Physiol. Regul. Integr. Comp. Physiol.* **314**, R533–R539 (2018).
68. A. A. da Silva, J. E. Hall, J. M. do Carmo, Leptin reverses hyperglycemia and hyperphagia in insulin deficient diabetic rats by pituitary-independent central nervous system actions. *PLoS One* **12**, e0184805 (2017).
69. T. Masaoka *et al*., Enhanced plasma ghrelin levels in rats with streptozotocin-induced diabetes. *FEBS Lett.* **541**, 64–68 (2003).
70. M. A. Rosas Fernández *et al*., Intermittent food restriction in female rats induces SREBP high expression in hypothalamus and immediately postfasting hyperphagia. *Nutrition* **48**, 122–126 (2018).
71. L. Penicaud, J. Le Magnen, Recovery of body weight following starvation or food restriction in rats. *Neurosci. Biobehav. Rev.* **4** (suppl. 1), 47–52 (1980).
72. E. Holeckova, P. Fabry, Hyperphagia and gastric hypertrophy in rats adapted to intermittent starvation. *Br. J. Nutr.* **13**, 260–266 (1959).
73. R. B. Harris, T. R. Kasser, R. J. Martin, Dynamics of recovery of body composition after overfeeding, food restriction or starvation of mature female rats. *J. Nutr.* **116**, 2536–2546 (1986).
74. A. G. Dulloo, J. Jacquet, L. Girardier, Poststarvation hyperphagia and body fat overshooting in humans: A role for feedback signals from lean and fat tissues. *Am. J. Clin. Nutr.* **65**, 717–723 (1997).
75. C. Sefton *et al*., Elevated hypothalamic glucocorticoid levels are associated with obesity and hyperphagia in male mice. *Endocrinology* **157**, 4257–4265 (2016).
76. J. Solomon, J. Mayer, The effect of adrenalectomy on the development of the obese-hyperglycemic syndrome in *ob-ob* mice. *Endocrinology* **93**, 510–512 (1973).
77. M. Saito, G. A. Bray, Adrenalectomy and food restriction in the genetically obese (*ob/ob*) mouse. *Am. J. Physiol.* **246**, R20–R25 (1984).
78. H. Makimura *et al*., Adrenalectomy reverses obese phenotype and restores hypothalamic melanocortin tone in leptin-deficient *ob/ob* mice. *Diabetes* **49**, 1917–1923 (2000).
79. J. S. Kang, J. D. Pilkington, D. Ferguson, H. K. Kim, D. R. Romsos, Dietary glucose and fat attenuate effects of adrenalectomy on energy balance in *ob/ob* mice. *J. Nutr.* **122**, 895–905 (1992).
80. H. Shimizu, K. Ohshima, G. A. Bray, M. Peterson, R. S. Swerdloff, Adrenalectomy and castration in the genetically obese (*ob/ob*) mouse. *Obes. Res.* **1**, 377–383 (1993).
81. K. M. Feldkircher, A. M. Mistry, D. R. Romsos, Adrenalectomy reverses pre-existing obesity in adult genetically obese (*ob/ob*) mice. *Int. J. Obes. Relat. Metab. Disord.* **20**, 232–235 (1996).
82. P. Naeser, Effects of adrenalectomy on the obese-hyperglycemic syndrome in mice (gene symbol *ob*). *Diabetologia* **9**, 376–379 (1973).
83. K. Clément *et al*., A mutation in the human leptin receptor gene causes obesity and pituitary dysfunction. *Nature* **392**, 398–401 (1998).
84. R. S. Ahima, J. S. Flier, Leptin. *Annu. Rev. Physiol.* **62**, 413–437 (2000).
85. I. S. Farooqi *et al*., Beneficial effects of leptin on obesity, T cell hyporesponsiveness, and neuroendocrine/metabolic dysfunction of human congenital leptin deficiency. *J. Clin. Invest.* **110**, 1093–1103 (2002).
86. M. Ozata, I. C. Ozdemir, J. Licinio, Human leptin deficiency caused by a missense mutation: Multiple endocrine defects, decreased sympathetic tone, and immune system dysfunction indicate new targets for leptin action, greater central than peripheral resistance to the effects of leptin, and spontaneous correction of leptin-mediated defects. *J. Clin. Endocrinol. Metab.* **84**, 3686–3695 (1999).
87. S. H. Chou *et al*., Leptin is an effective treatment for hypothalamic amenorrhea. *Proc. Natl. Acad. Sci. U.S.A.* **108**, 6585–6590 (2011).
88. E. Charmandari, N. C. Nicolaides, G. P. Chrousos, Adrenal insufficiency. *Lancet* **383**, 2152–2167 (2014).
89. R. Salvatori, Adrenal insufficiency. *JAMA* **294**, 2481–2488 (2005).
90. B. S. Berthon, L. K. MacDonald-Wicks, L. G. Wood, A systematic review of the effect of oral glucocorticoids on energy intake, appetite, and body weight in humans. *Nutr. Res.* **34**, 179–190 (2014).
91. P. A. Tataranni *et al*., Effects of glucocorticoids on energy metabolism and food intake in humans. *Am. J. Physiol.* **271**, E317–E325 (1996).
92. A. J. Li, Q. Wang, S. Ritter, Selective pharmacogenetic activation of catecholamine subgroups in the ventrolateral medulla elicits key glucoregulatory responses. *Endocrinology* **159**, 341–355 (2018).
93. V. Sergeyev, C. Broberger, O. Gorbatyuk, T. Hökfelt, Effect of 2-mercaptoacetate and 2-deoxy-D-glucose administration on the expression of NPY, AGRP, POMC, MCH and hypocretin/orexin in the rat hypothalamus. *Neuroreport* **11**, 117–121 (2000).
94. D. K. Sindelar *et al*., Neuropeptide Y is required for hyperphagic feeding in response to neuroglucopenia. *Endocrinology* **145**, 3363–3368 (2004).
95. M. A. Sacta, Y. Chinenov, I. Rogatsky, Glucocorticoid signaling: An update from a genomic perspective. *Annu. Rev. Physiol.* **78**, 155–180 (2016).
96. J. M. Resch *et al*., Aldosterone-sensing neurons in the NTS exhibit state-dependent pacemaker activity and drive sodium appetite via synergy with angiotensin II signaling. *Neuron* **96**, 190–206.e7 (2017).
97. F. L. Groeneweg, H. Karst, E. R. de Kloet, M. Joëls, Rapid non-genomic effects of corticosteroids and their role in the central stress response. *J. Endocrinol.* **209**, 153–167 (2011).
98. E. Gyengesi *et al*., Corticosterone regulates synaptic input organization of POMC and NPY/AgRP neurons in adult mice. *Endocrinology* **151**, 5395–5402 (2010).
99. M. Shibata *et al*., AgRP neuron-specific deletion of glucocorticoid receptor leads to increased energy expenditure and decreased body weight in female mice on a high-fat diet. *Endocrinology* **157**, 1457–1466 (2016).
100. S. Luquet, F. A. Perez, T. S. Hnasko, R. D. Palmiter, NPY/AgRP neurons are essential for feeding in adult mice but can be ablated in neonates. *Science* **310**, 683–685 (2005).
101. E. Gropp *et al*., Agouti-related peptide-expressing neurons are mandatory for feeding. *Nat. Neurosci.* **8**, 1289–1291 (2005).
102. E. van de Wall *et al*., Collective and individual functions of leptin receptor modulated neurons controlling metabolism and ingestion. *Endocrinology* **149**, 1773–1785 (2008).
103. R. J. Perry *et al*., Leptin mediates a glucose-fatty acid cycle to maintain glucose homeostasis in starvation. *Cell* **172**, 234–248.e7 (2018).